UDC 621.921.34:666.233
DOI dx.doi.org/10.17073/1997-308X-2022-4-67-83

Air-thermal oxidation of diamond nanopowders obtained by the methods of mechanical grinding and detonation synthesis

© 2022 г. **P.P. Sharin**[1], **A.V. Sivtseva**[1], **V.I. Popov**[2]

[1] Institute of Physical and Technical Problems of the North n.a. V.P. Larionov of Siberian Branch of Russian Academy of Sciences (SB RAS) under Federal Research Center «Yakutsk Scientific Center» of SB RAS, Yakutsk, Russia

[2] North-Eastern Federal University n.a. M.K. Ammosov, Yakutsk, Russia

Received 24.01.2022, revised 02.06.2022, accepted for publication 06.06.2022

Abstract: In this work, using the methods of *X*-ray phase analysis, transmission electron microscopy, *X*-ray photoelectron spectroscopy and Raman spectroscopy, the features of the impact of annealing in air within the temperature range of t = 200÷÷550 °C on the morphology, elemental and phase composition, chemical state and structure of primary particles of nanopowders obtained by grinding natural diamond and the method of detonation synthesis are studied. It is shown that heat treatment in air at given values of temperature and heating time does not affect the elemental composition and atomic structure of primary particles of nanopowders obtained both by the methods of detonation synthesis (DND) and natural diamond grinding (PND). Using XPS, Raman spectroscopy, and transmission electron microscopy, it has been found that annealing in air within the temperature range of 400—550 °C results in the effective removal of amorphous and graphite-like carbon atoms in the sp^2- and sp^3-states from diamond nanopowders by oxidation with atmospheric oxygen. In the original DND nanopowder, containing about 33.2 % of non-diamond carbon atoms of the total number of carbon atoms, after annealing for 5 h at a temperature of 550 °C, the relative number of non-diamond carbon atoms in the sp^2-state decreased to ~21.4 %. In this case, the increase in the relative number of carbon atoms in the sp^3-state (in the lattice of the diamond core) and in the composition of oxygen-containing functional groups ranged from ~39.8 % to ~46.5 % and from ~27 % to ~32.1 %, respectively. In the PND nanopowder, which prior to annealing contains about 10.6 % of non-diamond carbon atoms in the sp^2-state of the total number of carbon atoms, after annealing under the same conditions as the DND nanopowder, their relative number decreased to 7.1 %. The relative number of carbon atoms in the sp^3-state increased from 72.9 % to 82.1 %, and the proportion of carbon atoms in the composition of oxygen-containing functional groups also slightly increased from 10.2 % to 10.8 %. It is demonstrated that the annealing of PND and DND nanopowders in air leads to a change in their color, they become lighter as a result of oxidation of non-diamond carbon by atmospheric oxygen. The maximum effect is observed at a temperature of 550 °C and an annealing time of 5 h. In this case, the weight loss of PND and DND nanopowders after annealing was 5.37 % and 21.09 %, respectively. The significant weight loss of DND nanopowder compared to PND is primarily caused by the high content of non-diamond carbon in the initial state and the high surface energy of primary particles due to their small size.

Keywords: natural diamond nanopowder, detonation nanodiamond, thermal oxidation of nanopowders, morphology, elemental composition, atomic structure of diamond nanoparticles, chemical state of nanopowders, oxygen-containing functional groups.

Sharin P.P. — Cand. Sci. (Phys.-Math.), lead researcher of the Department of physicochemistry of the Institute of Physical and Technical Problems of the North n.a. V.P. Larionov of Siberian Branch of Russian Academy of Sciences (RAS) (677980, Russia, Rep. Sakha, Yakutsk, Oktyabrskaya str., 1). E-mail: psharin1960@mail.ru.

Sivtseva A.V. — researcher of the Department of material science of the Institute of Physical and Technical Problems of the North n.a. V.P. Larionov of Siberian Branch of RAS. E-mail: sianva@yandex.ru.

Popov V.I. — Cand. Sci. (Phys.-Math.), senior researcher of the scientific and technological laboratory «Graphene nanotechnologies» of the Physical and Technical Institute of the North-Eastern Federal University n.a. M.K. Ammosov (677000, Russia, Rep. Sakha, Yakutsk, Belinskii str., 58). E-mail: volts@mail.ru.

For citation: *Sharin P.P., Sivtseva A.V., Popov V.I.* Air-thermal oxidation of diamond nanopowders obtained by the methods of mechanical grinding and detonation synthesis. *Izvestiya Vuzov. Poroshkovaya Metallurgiya i Funktsional'nye Pokrytiya (Powder Metallurgy and Functional Coatings)*. 2022. Vol. 16. No. 4. P. 67—83 (In Russ.). DOI: dx.doi.org/10.17073/1997-308X-2022-4-67-83.

Термоокисление на воздухе нанопорошков алмазов, полученных механическим измельчением и методом детонационного синтеза

П.П. Шарин[1], **А.В. Сивцева**[1], **В.И. Попов**[2]

[1] Институт физико-технических проблем Севера (ИФТПС) им. В.П. Ларионова СО РАН при Федеральном исследовательском центре «Якутский научный центр» (ФИЦ ЯНЦ) СО РАН, г. Якутск, Россия

[2] Северо-Восточный федеральный университет им. М.К. Аммосова, г. Якутск, Россия

Статья поступила в редакцию 24.01.22 г., доработана 02.06.22 г., подписана в печать 06.06.22 г.

Аннотация: Методами рентгеноструктурного фазового анализа (РФА), просвечивающей электронной микроскопии (ПЭМ), рентгеновской фотоэлектронной спектроскопии (РФЭС) и спектроскопии комбинационного рассеяния исследованы особенности влияния отжига на воздухе в интервале температур t = 200÷550 °С на морфологию, элементный и фазовый составы, химическое состояние и структуру первичных частиц нанопорошков, полученных измельчением природного алмаза (ПНА) и методом детонационного синтеза (ДНА). Показано, что термообработка на воздухе при заданных значениях температуры и времени нагрева не оказывает влияние на элементный состав и атомную структуру первичных частиц нанопорошков, полученных как методом ДНА, так и методом ПНА. По результатам РФЭС, ПЭМ и спектроскопии комбинационного рассеяния установлено, что отжиг на воздухе при t = 400÷550 °С приводит к эффективному удалению из нанопорошков алмаза атомов аморфного и графитоподобного углерода в sp^2- и sp^3-состояниях путем окисления кислородом воздуха. В исходном нанопорошке ДНА, содержащем около 33,2 % атомов неалмазного углерода от общего количества атомов углерода, после отжига в течение 5 ч при t = 550 °С относительное количество атомов неалмазного углерода в sp^2-состоянии уменьшилась до ~21,4 %. При этом относительное количество атомов углерода в sp^3-состоянии (в решетке алмазного ядра) и в составе кислородсодержащих функциональных групп увеличилось соответственно с ~39,8 до ~46,5 % и с ~27 до ~32,1 %. В нанопорошке ПНА, содержащем до отжига около 10,6 % атомов неалмазного углерода в sp^2-состоянии от общего количества атомов углерода, после отжига при тех же условиях, что и для нанопорошка ДНА, их относительное количество снизилось до 7,1 %. При этом относительное количество атомов углерода в sp^3-состоянии повысилось с 72,9 до 82,1 %, также незначительно (с 10,2 до 10,8 %) возросла доля атомов углерода в составе кислородсодержащих функциональных групп. Показано, что отжиг на воздухе нанопорошков ПНА и ДНА приводит к изменению их цвета: в результате окисления неалмазного углерода кислородом воздуха они становятся более светлыми. Максимальный эффект наблюдается при температуре 550 °С и времени отжига 5 ч. При этом потери массы нанопорошков ПНА и ДНА после отжига составили, соответственно, 5,37 и 21,09 % — значительная потеря в массе нанопорошка ДНА обусловлена, в основном, высоким содержанием в исходном состоянии неалмазного углерода и высокой поверхностной энергией первичных частиц вследствие их малого размера.

Ключевые слова: нанопорошок природного алмаза, детонационный наноалмаз, термическое окисление нанопорошков, морфология, элементный состав и атомная структура наночастиц алмаза, химическое состояние нанопорошков, кислородсодержащие функциональные группы.

Шарин П.П. — канд. физ.-мат. наук, вед. науч. сотр. отдела физикохимии материалов и технологий ИФТПС им. В.П. Ларионова СО РАН (677980, Респ. Саха (Якутия), г. Якутск, ул. Октябрьская, 1).
E-mail: psharin1960@mail.ru.

Сивцева А.В. — науч. сотр. отдела материаловедения ИФТПС СО РАН.
E-mail: sianva@yandex.ru.

Попов В.И. — канд. физ.-мат. наук, ст. науч. сотр. учебной научно-технологической лаборатории «Графеновые нанотехнологии» Физико-технического института Северо-Восточного федерального университета им. М.К. Аммосова (677000, Респ. Саха (Якутия), г. Якутск, ул. Белинского, 58).
E-mail: volts@mail.ru.

Для цитирования: *Шарин П.П., Сивцева А.В., Попов В.И.* Термоокисление на воздухе нанопорошков алмазов, полученных механическим измельчением и методом детонационного синтеза. *Известия вузов. Порошковая металлургия и функциональные покрытия.* 2022. Т. 16. No. 4. С. 67—83. DOI: dx.doi.org/10.17073/1997-308X-2022-4-67-83.

Introduction

Diamond nanoparticles are a unique class of nano-sized materials with a variable structure and unstable physical and chemical properties [1—4]. Regardless of the method of obtaining, each primary particle of diamond nanopowders consists of a diamond core having a cubic crystal lattice and being surrounded by a shell with a complex structure formed predominantly of non-diamond carbon and non-carbon impuri-

ties [4—6]. Due to the ultra-small size and, consequently, the high proportion of surface atoms with partially non-compensated electronic bonds, the primary particles of diamond nanopowders exhibit enormous surface activity, therefore in addition to segments of non-diamond carbon structures, the shell contains various functional groups, including C—H, oxygen-containing groups [7—9] imparting various physicochemical properties to it.

At present, diamond nanopowders are used as various functional components in polishing compounds [10], lubricating oils [1, 11], composite materials [12], elements of microelectronics [13, 14], as well as selective adsorbents and catalysts [15, 16]. A large number of other potential applications of nanodiamonds, including their application as drug carriers [17, 18], immobilizers of biologically active substances, a sorbent for the purification of blood, lymph, etc. [19, 20], are still at the examination stage. Most of these promising applications are hindered by the impossibility of obtaining diamond nanoparticles with controlled and reproducible surface chemistry depending on (being determined by) the extreme conditions of their production and the purification methods being used. The relative content of non-diamond carbon, the composition of functional groups and impurity atoms of primary particles of diamond nanopowders produced even by one manufacturer may differ from one batch to another [1—3].

In this context, the study of the processes of modification of diamond nanoparticles constitutes an urgent task, the solution of which will reveal the regularities of changes in their morphology, composition and structure under directed external influence, which contributes to obtaining diamond nanoparticles with controlled and reproducible properties, thus being important for their high-tech applications including biology, medicine etc. In works [4, 7, 21—23], the efficient and environmentally friendly method of purification of non-diamond carbon and impurities as well as modification of detonation synthesis diamond nanopowders by means of thermal oxidation with atmospheric oxygen without significant losses of diamond component are proposed and studied. Despite a significant number of works devoted to the study of thermal annealing in air, many issues and aspects of the formation of the composition and content of functional structures impacting the chemistry of diamond nanopowders are still unresolved and require clarification and additions.

The purpose of this paper is to study the features of the impact of modification by oxidation with atmospheric oxygen within the temperature range of 200—550 °C on the morphology, elemental and phase composition, chemical state and structure of primary particles of nanopowders obtained by natural diamond grinding and by the method of detonation synthesis.

The subjects, methodology and methods of research

The samples of diamond nanopowders, obtained by two methods — the mechanical grinding of natural diamond and detonation synthesis from trinitrotoluene, were taken for the research. The procedure for obtaining nanopowders from natural diamond (PND) and their chemical purification are described extensively in work [6]. Highly purified nanopowder was used as samples of detonation synthesis nanodiamond (DND) of UDA-S-GO grade produced by Federal Research and Production Center «Altai» (Biysk).

A total of 12 samples of nanopowders, namely 6 samples of PND and DND were prepared. All samples of PND and DND were prepared from the same batch of the corresponding types of nanopowders. The staged heating of samples in air at atmospheric pressure was carried out as follows. All 12 samples of nanopowders were poured into separate ceramic corundum cups placed in a furnace chamber and heated in air at the following set temperature values (°C): 200, 300, 400, 500, and 550. After being held for 1 hour at each given temperature value, one sample of PND and DND was removed from the furnace for subsequent research, and the remaining samples were retained in the furnace chamber, the temperature of which was increased by the next given value at a rate of ~50 °C/min. Thus, the total time of staged heating of samples of PND and DND nanopowders in air at a temperature of 200 °C was 1 h, at a temperature of 300 °C — 2 h, at a temperature of 400 °C — 3 h, at a temperature of 500 °C — 4 h, and temperature of 550 °C — 5 h.

Morphological and structural characteristics of primary particles of nanopowders were studied by the methods of scanning electron microscopy (SEM) by means of JSM-6480LV instrument (JEOL, Japan) and high-resolution transmission electron microscopy (TEM) by means of «Titan 80-300» instrument (FEI, USA) with the following resolution: STEM; HREM ~0,08 nm. Digital processing of TEM images (Fourier transform, Fourier filtering, the determination of interplanar distances by FFT spectra) was performed using GMS-2.3.2 software package (GATAN, USA). The study of the phase composition and structural parameters of the samples of primary particles of nanopowders

was performed by means of «D8 Discover» powder diffractometer available from «Bruker» Company (USA) in CuK_α radiation (λ = 1.54 Å). *X*-ray diffraction measurements were performed in the range of 2θ angles from 17° to 96°. The measurement data were processed and analyzed using Microcal Origin and Crystallographica Search Match applications.

The elemental and phase compositions, the chemical state of primary particles of nanopowders were studied by the methods of *X*-ray photoelectron spectroscopy (XPS) and Raman spectroscopy. XPS measurements were performed by means of SPECS photoelectron spectrometer (Germany) using PHOIBOS-150-MCD-9 hemispherical analyzer and FOCUS-500 *X*-ray monochromator (AlK_α aradiation, hv = 1486.74 eV, 200 W). Binding energy scale (E_{bind}) was precalibrated by the position of the peaks of the core levels Au4f$_{7/2}$ (84.00 eV) and Cu2p$_{3/2}$ (932.67 eV). The samples of nanopowders were applied onto a double-sided copper conductive tape 3M (USA). The panoramic spectra were recorded at a transmission energy of the analyzer of 50 eV, and certain spectral areas were recorded at the energies of 10 or 20 eV. The determination of the relative content of elements on the samples of nanopowders and their atomic ratios was performed in accordance with the integral intensities of photoelectron lines (C1s, O1s and N1s) adjusted for the corresponding atomic sensitivity coefficients [24].

The Raman spectra (Raman) of nanopowder samples were studied using Solar TII Raman spectrometer being an integral part of Integra Spectra measuring complex (NT-MDT, JSC, Zelenograd). This spectrometer is equipped with a microscope with an objective of 100$^\times$ with a number aperture of NA = 0.7, a TV camera and a cooled CCD detector (–70 °C). Laser radiation with the wavelengths of 473, 532, and 632 nm was used for Raman spectra excitation. When registering Raman spectra, a diffraction grating with a density of 600 lines/mm was used in the spectrometer. The Raman spectra of the samples were measured in the signal accumulation mode at room temperature.

The specific surface area of the samples was determined by BET method (Brunauer—Emmett—Teller) according to measurements of the low-temperature adsorption of nitrogen molecules (77 K) using SORBI-MS instrument (Meta, JSC, Novosibirsk) equipped with GSO 7912-2001 standard sample (S_{sp} = 98.42 m^2/g) developed at G.K. Boreskov Institute of Catalysis, SB RAS (Novosibirsk). The density of diamond nanopowders was estimated by the pycnometric method.

Results and discussions

Table 1 provides the basic physical characteristics of the original PND and DND nanopowders. The pycnometric densities of both nanopowders are significantly lower than the theoretical density of diamond (3.5154 g/cm^3) and the density of massive natural diamond crystals, which, as it is known, varies in the range of 3.30—3.60 g/cm^3 depending on their impurity content [25].

In the daylight, dry PND nanopowder in its initial state exhibits a light gray color (Fig. 1, *a*), while after annealing in air at a temperature of 550 °C for 5 h, the color of the sample changed and became almost white with a slightly grayish tint (Fig. 1, *c*). After annealing in air under the same conditions, the dark brown color of the original dry nanopowder of DND sample (Fig. 1, *b*) changed to light gray (Fig. 1, *d*).

***X*-ray phase analysis.** 3 clear lines, corresponding to *X*-ray diffraction on (111), (220) and (311) planes of the crystal lattice of the diamond core of the primary particles of PND and DND nanopowders, were identified on the diffraction spectra in the studied range of angles 2θ ~17÷96 deg. (Fig. 2). The ratios of intensity of three diffraction peaks $I_{111} : I_{220} : I_{311}$ for all the samples of PND and DND, including the samples subjected to staged heating in air, are about 100 : 51 : 18 and 100 : 21 : 12, respectively.

There is a line observed in the spectrum of the original DND sample in the range of 2θ ~ 18÷28 deg. (spectrum *1* in Fig. 2, *a*), which is caused by the dif-

Table 1. **Main physical characteristics of diamond nanopowders**

Таблица 1. Основные физические характеристики алмазных нанопорошков

Powder	Size, nm (*X*-ray phase analysis)	Pycnometric densities, g/cm^3	Specific surface area, m^2/g	Non-combustible residue, %
PND	19.88 ± 3.0	3.05	32.98 ± 2.0	0.95
DND	4.98 ± 0.74	2.95	339.5 ± 20	1.1

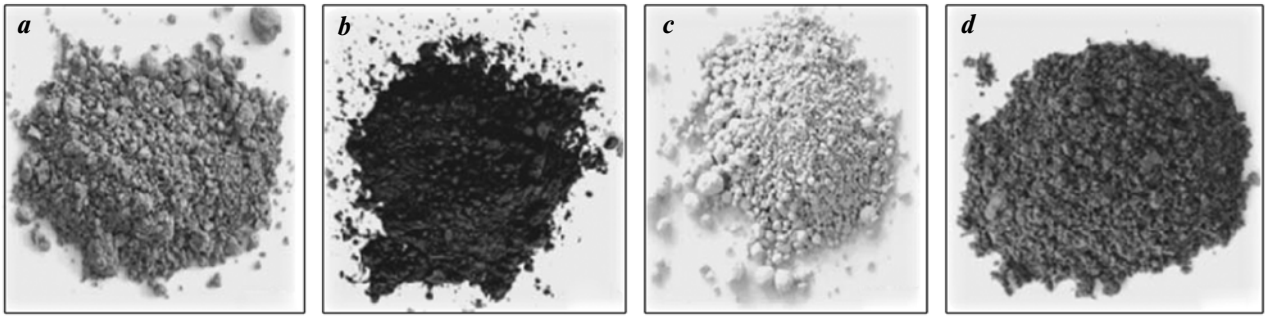

Fig. 1. The photographs of samples of PND and DND nanopowders in the initial state (***a***, ***b***) and after annealing in air for 5 h at a temperature of 550°C (***c***, ***d***)

Рис. 1. Фотографии образцов нанопорошков ПНА и ДНА в исходном состоянии (***a***, ***b***) и после отжига на воздухе в течение 5 ч при температуре 550 °С (***c***, ***d***)

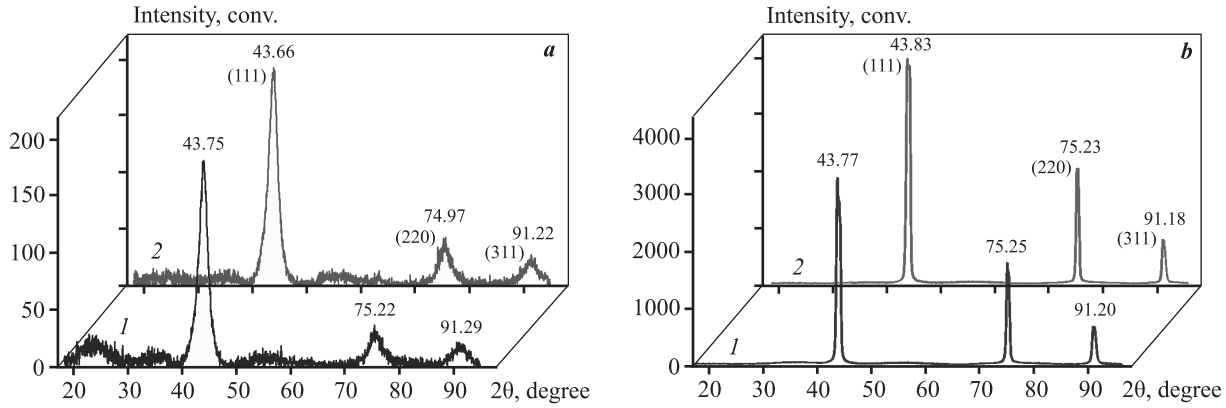

Fig. 2. *X*-ray diffraction spectra of DND nanopowders (***a***) and PND nanopowders (***b***) before annealing (***1***) and after annealing in air at a temperature of 550 °C (***2***)

Рис. 2. Рентгеновские дифракционные спектры нанопорошков ДНА (***a***) и ПНА (***b***) до отжига (***1***) и после отжига на воздухе при температуре 550 °С (***2***)

fuse scattering of *X*-rays from formations without long-range order. The presence of such a line in the spectrum is commonly associated with amorphous structural groups consisting mainly of non-diamond carbon and located around the diamond core and in the space between the adjacent primary particles of the nanopowder. [21, 26]. While in the spectrum of the DND sample (spectrum *2* in Fig. 2, *a*), subjected to heating in air, such a line is virtually absent, or, upon annealing in air, the content of amorphous formations of non-diamond carbon decreased to such an amount that is not detectable by *X*-ray phase analysis. Fig. 2 also reveals that the diffraction peaks of the samples of both nanopowders are broadened, upon that the ones of DND are much more broadened compared to the ones of PND due to the smaller size of its crystallites.

It is known that the broadening of the diffraction lines of any powder made of crystalline grains can be contributed by secondary microstresses in their crystals [27]. In a number of works [3, 5, 28], it was experimentally demonstrated that in the case of nanodispersed diamond particles, the contribution of secondary microstresses is insignificant [28]. This is explained by the fact that any microstresses in crystallites caused by thermal or mechanical impact are efficiently relaxed due to the combination of high-modulus of diamond with the nanoscale of its particles [6]. In this context, the line broadening in the diffraction spectrum is primarily contributed by the small size of nanodiamond crystallites; therefore, when calculating the size of the coherent scattering region (D_{CSR}), which essentially corresponds to the size of the diamond core of primary

particles of nanopowders (without taking into account their shells), we used a simplified formula $D_{CSR} = \lambda/(\beta\cos\theta)$.

The data provided in Table 2 suggest that the physical broadening (β) of the diffraction lines of DND samples (the original ones and the ones heat-treated in air), depending on the value of the heating temperature, is on average approximately 3.9 times higher than the line broadening of PND samples. The comparative analysis of the angles of maxima of diffraction lines, interplanar spacings, and physical broadening for the original samples and the PND and DND samples subjected to annealing in air reveals that heat treatment at the temperatures and heating duration specified in the experiment does not impact the structural state of primary particles of nanopowders of both DND and PND.

The elemental composition and chemical state of the samples. Panoramic *X*-ray photoelectron spectra of DND and PND samples before heating and after annealing in air at a temperature of 550 °C provide general information on the chemical composition of nanopowder samples and the presence of impurities or contaminants in them. (Fig. 3).

It is worth noting that XPS method, as applied to the nanopowder samples under study, provides information not only from the surface of their primary particles, but also from the entire volume of the ones

Table 2. **The values of heating temperature (*t*), angles of maximum of diffraction lines (2θ), interplanar distances (d_{hkl}), physical broadening (β) and the size of coherent scattering regions (D_{CSR}) samples of PND and DND nanopowders before and after the staged heat treatment in air**

Таблица 2. Значения температуры нагрева (*t*), углов максимума дифракционных линий (2θ), межплоскостных расстояний (d_{hkl}), физического уширения (β) и размера областей когерентного рассеяния ($D_{ОКР}$) образцов нанопорошков ПНА и ДНА до и после ступенчатой термообработки на воздухе

t, °C	Miller indices	PND				DND			
		2θ, deg.	d_{hkl}, Å	β, deg.	D_{CSR}, nm	2θ, deg.	d_{hkl}, Å	β, deg.	D_{CSR}, nm
Orig.	(111)	43.77	2.067	0.66	14.08	43.75	2.068	2.23	4.16
	(220)	75.25	1.262	0.43	25.48	75.22	1.263	2.00	5.44
	(311)	91.20	1.079	0.61	20.08	91.29	1.078	2.30	5.36
200	(111)	43.79	2.066	0.60	15.49	43.82	2.065	2.26	4.11
	(220)	75.26	1.262	0.43	25.41	75.25	1.262	1.99	5.47
	(311)	91.22	1.078	0.65	18.96	90.94	1.081	2.30	5.34
300	(111)	43.78	2.067	0.55	16.92	43.68	2.071	2.14	4.34
	(220)	75.23	1.262	0.48	22.74	75.34	1.261	2.14	5.10
	(311)	91.21	1.078	0.61	20.33	91.00	1.080	2.20	5.59
400	(111)	43.80	2.066	0.65	14.20	43.68	2.071	2.18	4.25
	(220)	75.24	1.262	0.43	25.34	75.20	1.263	2.05	5.31
	(311)	91.20	1.078	0.60	20.68	91.50	1.076	2.10	5.88
500	(111)	43.79	2.066	0.64	14.42	43.57	2.076	2.12	4.38
	(220)	75.25	1.262	0.43	25.34	74.91	1.267	2.10	5.17
	(311)	91.17	1.079	0.60	20.68	91.13	1.079	2.04	6.05
550	(111)	43.83	2.065	0.65	14.23	43.66	2.072	2.11	4.40
	(220)	75.23	1.262	0.42	25.91	74.97	1.266	1.98	5.49
	(311)	91.18	1.079	0.60	20.50	91.22	1.078	2.09	5.90

or a significant part of it, since the mean free path of electrons (λ ~ 3 nm) is comparable to or slightly less than the average size of the studied primary particles of DND and PND nanopowders. Taking into account the fact that about 95 % of the informative signal in XPS comes from a depth of 3λ, the depth of analysis for carbon constitutes ~ 9÷10 nm. In Fig. 3, *a*, it can be seen that the spectra of the original samples of both nanopowders contain the lines being specific for carbon (C1s and C KVV) and oxygen (O1s and O KLL). Besides, the spectrum of the DND sample includes a nitrogen line (N1s), while the spectrum of the PND sample includes additional low-intensity peaks of titanium and sodium (practically at the level of noises). No other elements were found in all samples of nanopowders within the sensitivity of XPS method. The photoelectron spectra of DND and PND samples subjected to heat treatment in air at a temperature of 550 °C (Fig. 3, *b*) contain the same lines as the corresponding original samples. Table 3 provides the results of measurements of the relative content of basic elements (C, O and N), as well as the ratio of their atomic concentrations in the samples of DND and PND nanopowders.

The relative content of elements in the samples of nanopowders and their atomic ratios were determined by the integral intensities of photoelectron lines adjusted for the corresponding atomic sensitivity coefficients [24].

According to Table 3, the ratio of the number of oxygen atoms and carbon atoms is practically the same for the particles of PND and DND nanopowders.

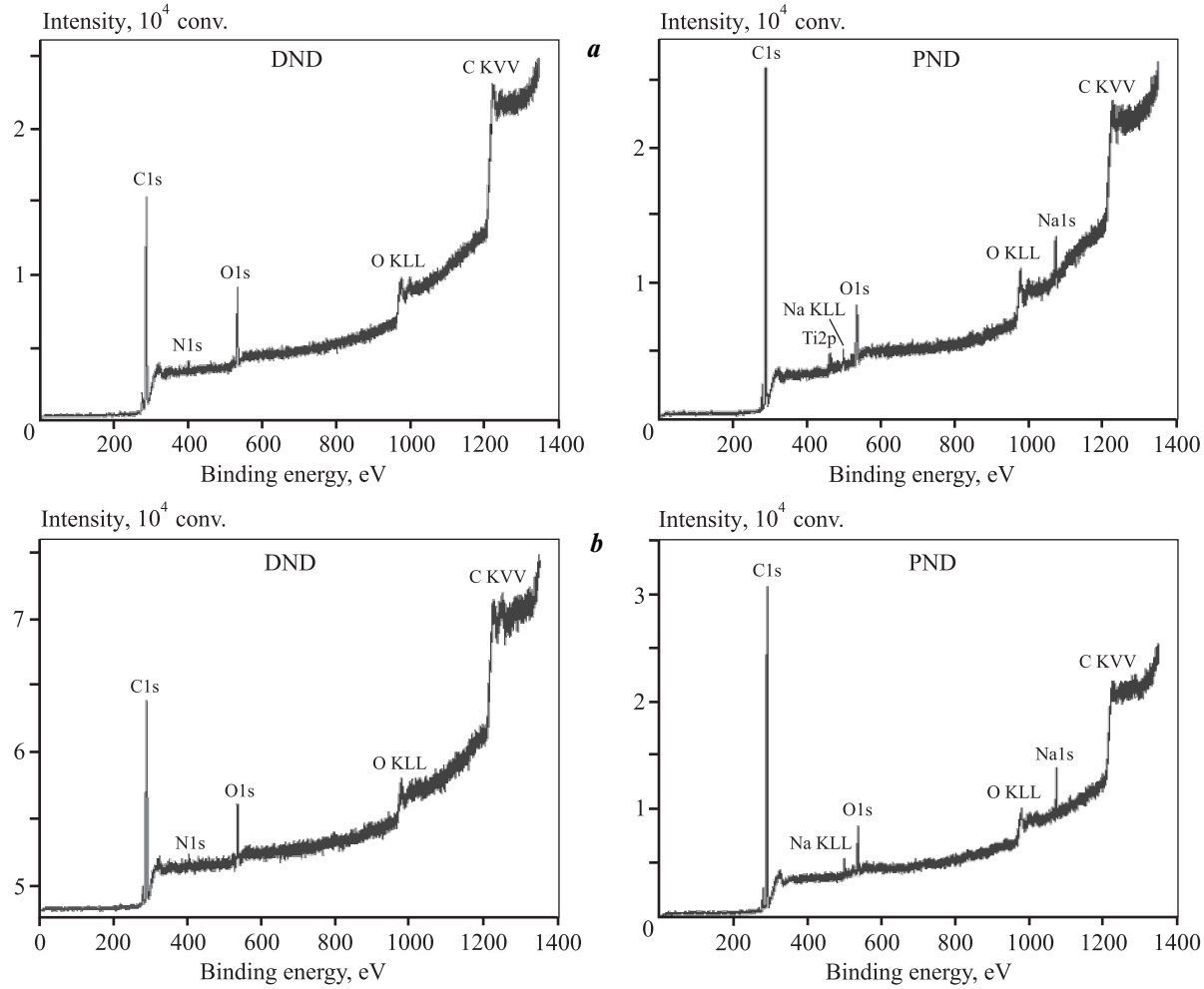

Fig. 3. The panoramic *X*-ray photoelectron spectra of DND and PND samples before heating (***a***) and after annealing in air at a temperature of 550 °C (***b***)

Рис. 3. Обзорные рентгеновские фотоэлектронные спектры образцов ДНА и ПНА до нагрева (***a***) и после отжига на воздухе при температуре 550 °C (***b***)

Table 3. **The relative content of elements in PND and DND samples and their atomic ratios**

Таблица 3. Относительное содержание элементов в образцах ПНА и ДНА и их атомные соотношения

t, °C	PND					DND				
	C	O	N	O/C	N/C	C	O	N	O/C	N/C
Orig.	90.6	9.4	—	0.10	—	89.4	9.1	1.5	0.10	0.02
400	90.8	9.2	—	0.10	—	89.0	9.5	1.5	0.11	0.02
500	91.2	8.8	—	0.10	—	89.4	9.0	1.6	0.10	0.02
550	90.8	9.2	—	0.10	—	90.6	7.8	1.6	0.19	0.02

For a detailed analysis, the main lines of C1s carbon, O1s oxygen, and N1s nitrogen were decomposed into separate spectral components using XPSPeak 4.1 software [29].

Fig. 4 shows that the carbon C1s lines of both nanopowder samples consist of separate spectral components, indicating that the carbon within the samples appears in 4 different chemical states. An analysis of binding energies of individual components in C1s spectra of both samples allows to conclude that the most intensive peaks with binding energies of 285.3 ± 0.2 eV correspond to sp^3-hybridized carbon forming a diamond crystal lattice [7, 30—33].

The binding energies of peaks of 284.1 ± 0.1 eV are specific for carbon atoms in the sp^2-state (graphite-like carbon atoms) [30—33]. The peaks with the binding energies of 286.6 eV correspond to carbon atoms in the composition of hydroxyl and ether groups (C—OH, C—O—C) [30—33]. The least intensive lines with the binding energies of 287.9 ± 0.3 eV characterize the states of carbon atoms in the composition of carboxyl groups (O=C—O, COOH). Table 4 provides relative contributions of each state of carbon atoms to the total C1s spectrum and sp^2/sp^3 ratio for all measured samples. According to Table 4, in the original sample of PND nanopowder, about 79.2 % of the total number of carbon atoms are in the sp^3-state. ~10.6 % of the total number of carbon atoms correspond to graphite-like carbon atoms in the sp^2-hybridized state, while other carbon atoms are in the composition of hydroxyl (or ether) (~8.0 %) and carboxyl (~2.2 %) groups.

The original sample of DND nanopowder, 33.2 % of the total number of carbon atoms are graphite-like carbon atoms in the sp^2-hybridized state. The carbon atoms in the sp^3-hybridized state account for ~39.8 %, while other carbon atoms are in the composition of hydroxyl (or ether) (~24.8 %) and carboxyl (~2.2 %) groups. Table 4 also shows that as the temperature (starting from 400 °C) and the time of annealing in air increases, the content of non-diamond carbon atoms in the sp^2-hybridized state both in PND samples and in DND samples gradually decreases as a result of air oxidation, while the proportion of carbon atoms in the sp^3-hybridized state increases.

Fig. 5 shows O1s oxygen spectra of the samples of nanopowders measured before heating and after it (t = 550 °C). It can be seen that O1s spectra of DND and PND samples contain various oxygen-containing functional groups, which are commonly localized on the surface of carbon materials, including diamond nanopowders. According to the literature data, the peaks of oxygen atoms in the carbonyl groups of ketones, aldehydes and quinones are in the range of binding energies of ~531.3÷531.5 eV [34—36]. The binding energy of 532.6 eV is characteristic of peaks of oxygen in the composition of phenolic [34] and hydroxyl groups [35], as well as carbonyl oxygen in esters and carboxylic anhydrides [35]. The peaks of oxygen with the binding energy of 533.8 eV correspond to the non-carbonyl atom of oxygen in esters or anhydrides and carboxyl group [34, 36, 37]. The peaks of oxygen with the binding energy of 530 eV can be attributed to oxygen in the composition of inorganic compounds [35]. The relative contributions of different states of oxygen atoms to the total O1s spectrum in all measured PND and DND samples are provided in Table 5.

Table 5 shows that the PND samples annealed in air exhibit a noticeable tendency to an increase in the proportion of oxygen atoms in the composition of ester, carbonyl, and carboxyl functional groups compared to the initial state, while the DND samples annealed in air exhibit a somewhat decrease in the proportion of oxygen atoms of the hydroxyl and carbonyl groups in the composition of ester, anhydride and carboxyl groups compared to the original sample.

A certain increase in the fraction of oxygen atoms of the non-carbonyl group is also noticeable only in the composition of carboxyl, anhydride, and ester groups in DND samples after annealing. The analysis of the binding energies of spectral components presented in the spectrum of main line N1s in Fig. 6 allows

Table 4. **The contribution of carbon states (%) to the total spectrum of C1s in PND and DND samples before their annealing and after heating in air at different temperatures**

Таблица 4. Вклад состояний углерода, %, в суммарный спектр C1s в образцах ПНА и ДНА до их отжига и после нагрева на воздухе при разных значениях температуры

t, °C	PND					DND				
	sp^2	sp^3	C—O, C—O—C	COOH	sp^2/sp^3	sp^2	sp^3	C—O, C—O—C	COOH	sp^2/sp^3
Orig.	10.6	79.2	8.0	2.2	0.13	33.2	39.8	24.8	2.2	0.83
400	10.1	78.9	8.5	2.5	0.13	31.7	38.9	25.1	4.3	0.81
500	8.2	81.5	8.4	1.9	0.10	29.8	42.8	23.2	4.2	0.70
550	7.1	82.1	9.1	1.7	0.09	21.4	46.5	27.8	4.3	0.46

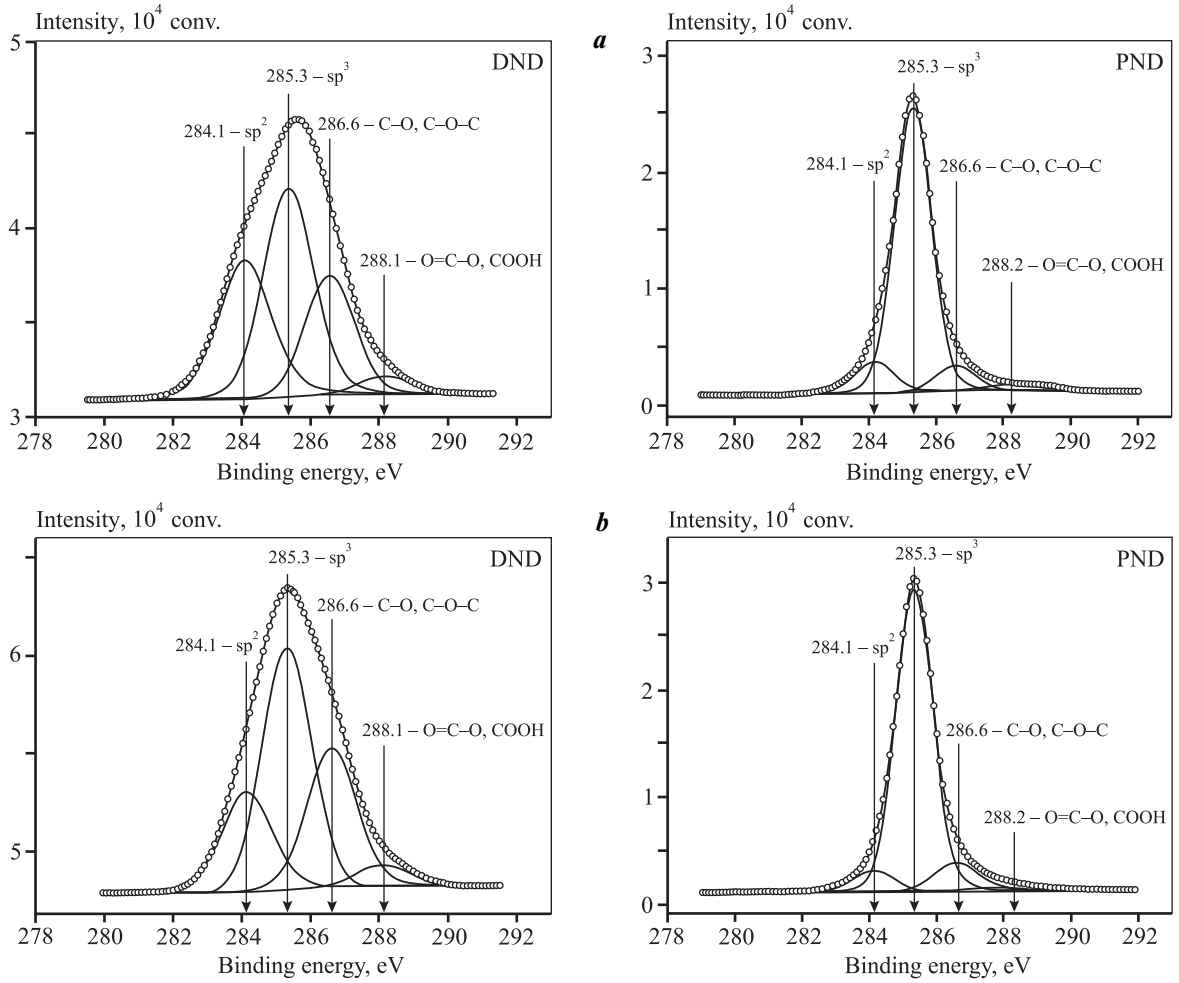

Fig. 4. The spectra of C1s carbon of DND and PND samples before heating (***a***) and after annealing in air at a temperature of 550 °C (***b***)

Рис. 4. Спектры углерода C1s образцов ДНА и ПНА до нагрева (***a***) и после отжига на воздухе при температуре 550 °C (***b***)

Table 5. **The contribution of the states of oxygen atoms (%) to the total spectrum of O1s**

Таблица 5. Вклад состояний атомов кислорода, %, в суммарный спектр O1s

t, °C	PND				DND			
	O=C—O—C, —C—OH	—C=O	—O—C=O	NaOH + TiO_2	O=C—O—C, —C—OH	—C=O	—O—C=O	NaOH + TiO_2
Orig.	36.7	18.6	14.2	30.5	64.6	27.7	7.7	—
400	46.8	21.6	16.7	14.9	58.6	31.0	10.4	—
500	49.3	21.9	16.6	12.2	57.6	29.4	12.9	—
550	49.9	21.7	21.1	7.3	55.2	27.0	17.8	—

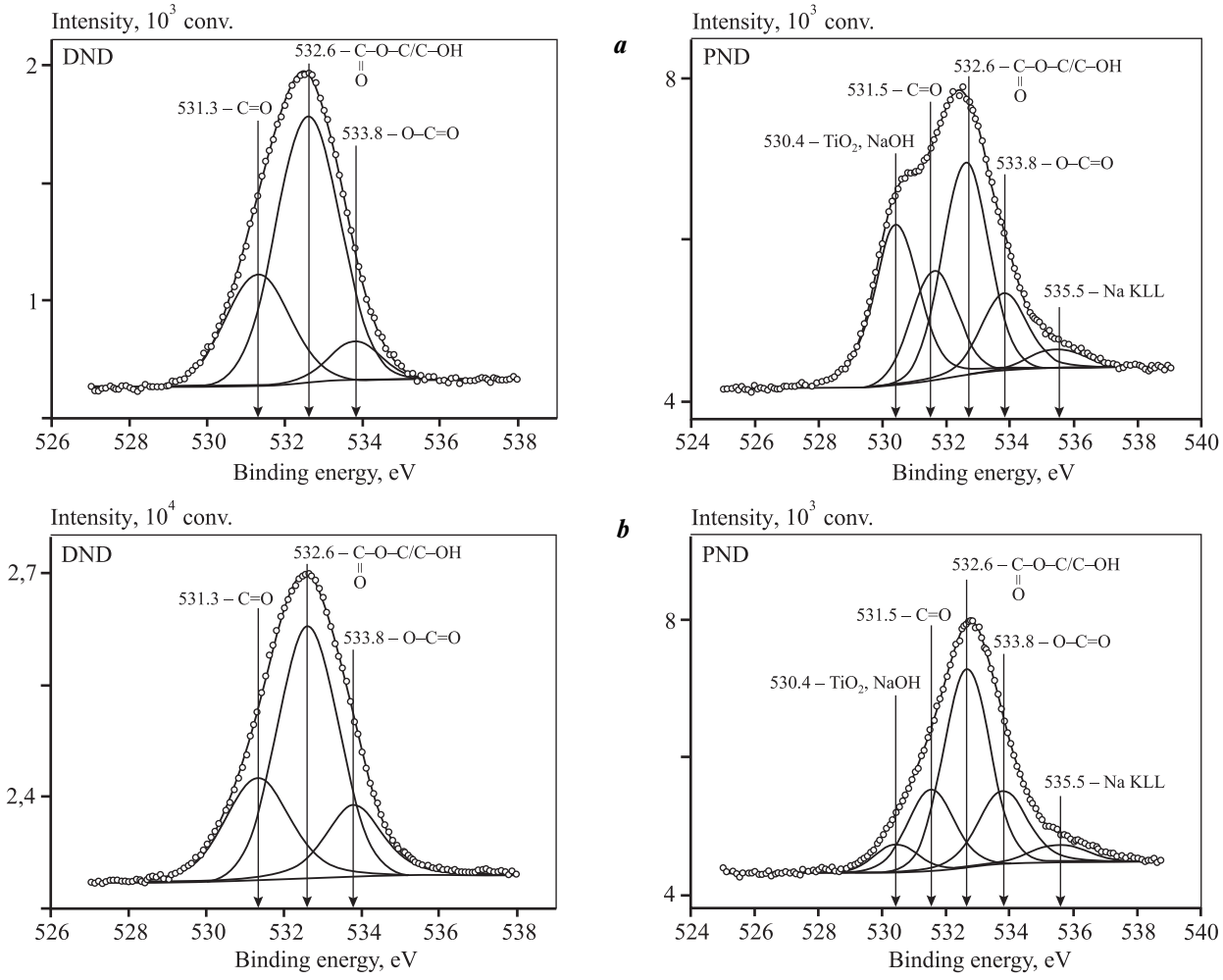

Fig. 5. The spectra of O1s oxygen of the samples of DND and PND nanopowders before heating (***a***) and after annealing in air at a temperature of 550 °C (***b***)

Рис. 5. Спектры кислорода O1s образцов нанопорошков ДНА и ПНА до нагрева (***a***) и после отжига на воздухе при температуре 550 °C (***b***)

to suggest that nitrogen is present on the surface in the composition of the following functional groups: 398.6 eV —C—N=C and 399.6 eV — C—N—C. Peak with the binding energy value of 402.8 ± 0.1 eV may belong to oxidized nitrogen (NO_x).

The contribution of nitrogen states in N1s spectra of the studied samples is provided in Table 6. The analysis of the binding energies of spectral components presented in N1s spectrum allows to suggest that nitrogen is present on the surface in the composition of

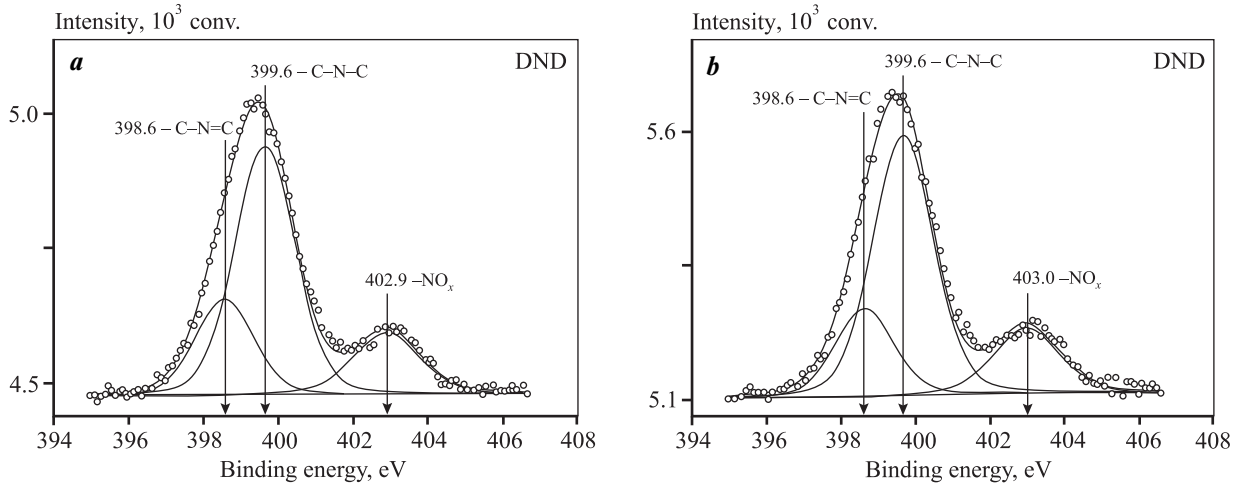

Fig. 6. The main lines of N1s nitrogen of the samples of DND nanopowder before heating (***a***) and after annealing in air at a temperature of 550 °C (***b***)

Рис. 6. Остовные линии азота N1s образцов нанопорошка ДНА до нагрева (***a***) и после отжига на воздухе при температуре 550 °C (***b***)

Table 6. **The contribution of the states of nitrogen atoms (%) to the total spectrum of N1s in DND samples**

Таблица 6. Вклад состояний атомов азота, %, в суммарный спектр N1s в образах ДНА

t, °C	C—N=C	C—N—C	NO_x
Orig.	27.3	55.6	17.1
400	25.2	57.5	17.3
500	22.3	60.4	17.3
550	21.3	61.3	17.4

the following functional groups: 398.6 eV —C—N=C and 399.6 eV — C—N—C. Peak with the binding energy value of 402.8 ± 0.1 eV may belong to oxidized nitrogen (NO_x).

Transmission electron microscopy. Fig. 7 shows the images of the structure of primary particles of DND and PND nanopowder samples in their initial state and after annealing in air at a temperature of 550 °C.

The interplanar distances of the crystals of the diamond core of the primary particles of nanopowders are distinctly visible in all the high-resolution images in Fig. 7. Both in DND nanopowder and in PND nanopowder, the shells consisting mainly of graphite-like carbon in sp^2-hybridized state and amorphous carbon in sp^3-state are clearly visible together with the cores of primary particles [4, 7]. The space between the adjacent primary particles is also filled with formations of non-diamond carbon and segments of amorphous carbon in sp^3-hybridized state (see Fig. 7). The comparative analysis of high-resolution images of primary DND and PND particles obtained before annealing and after heating in air in the temperature range of 400—550 °C is indicative of a noticeable decrease in non-diamond carbon both on the shells surrounding the cores of primary particles and in the space between the adjacent primary particles.

Thus, the results obtained by direct TEM observation are in qualitative line with the analysis data established on the basis of XPS measurements of C1s carbon, which show that the relative content of graphite-like carbon atoms in the sp^2-hybridized state decreases as a result of their being oxidized with atmospheric oxygen upon annealing of nanopowder samples at a temperature above 400 °C (see Table 4). A decrease in the relative content of non-diamond carbon in the samples during annealing in air as a result of oxidation is also observed in the Raman spectra of PND and DND nanopowders.

Raman spectroscopy. Fig. 8 shows the normalized Raman spectra (RS) of PND and DND nanopowders in their states before and after annealing (in air at t = 550 °C). It can be observed that the Raman spectra of the samples of PND and DND nanopowders in their initial state and after annealing differ significantly (see Fig. 8). Thus, in the Raman spectrum of PND sample, *D* line being the line of low-ordered carbon in sp^2-state, from which a sharp diamond peak, caused by the vibrations of carbon atoms in the sp^3-state, emerges at a frequency about 1331 cm^{-1}, and *G* line being the line

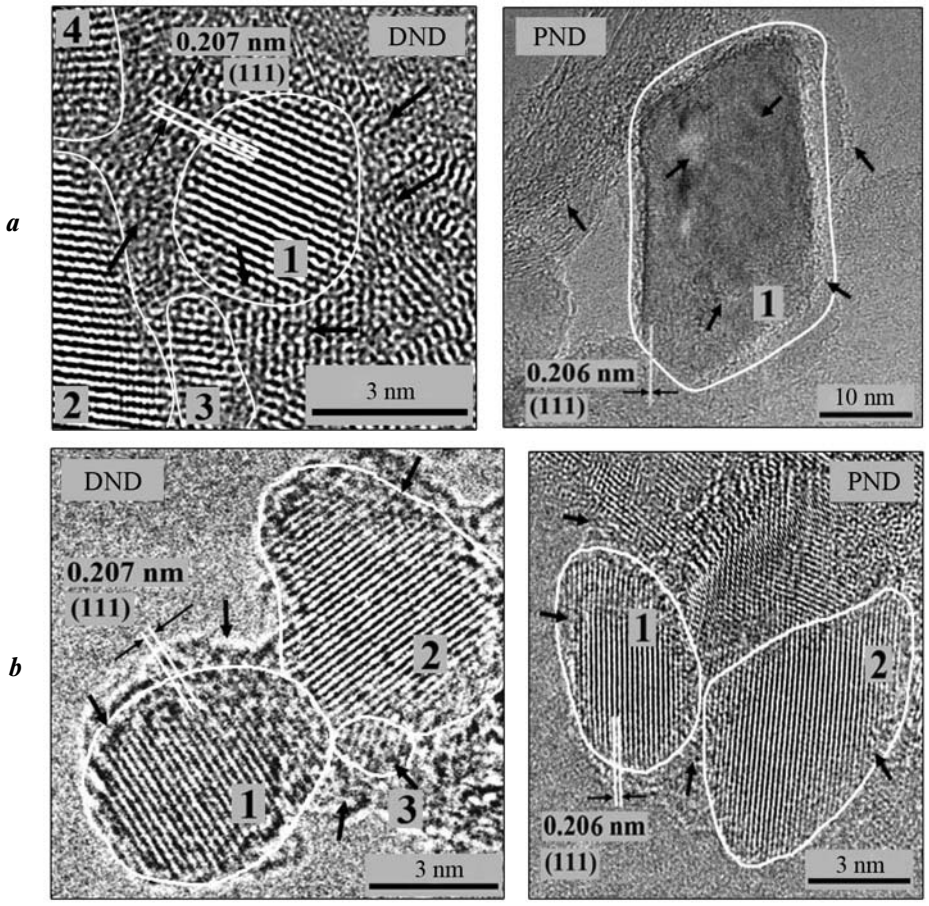

Fig. 7. The high-resolution images of primary particles of the samples of DND and PND nanopowders before annealing (***a***) and after heating in air at a temperature of 550 °C (***b***)

The numbers indicate the crystalline cores of diamond of primary particles of nanopowders, the arrows indicate the segments of graphite-like formations of carbon in the sp^2-state and amorphous carbon in the sp^3-state

Рис. 7. Изображения высокого разрешения первичных частиц образцов нанопорошков ДНА и ПНА до отжига (***a***) и после нагрева на воздухе при температуре 550 °C (***b***)

Цифрами помечены кристаллические ядра алмаза первичных частиц нанопорошков; стрелками обозначены фрагменты графитоподобных образований из углерода в sp^2-состоянии и аморфного углерода в sp^3-состоянии

of graphite, occupying the frequency range of 1400—1700 cm^{-1} with a center at 1577 cm^{-1}, decreased noticeably after annealing. In the Raman spectrum of DND sample before annealing, the diamond peak hardly stands out against the background of the intense broad *D* line of low-ordered carbon in sp^2-state, while after annealing the diamond peak is clearly observed at a frequency centered at about 1328 cm^{-1}. These changes in the Raman spectra are indicative of the fact that the proportions of non-diamond carbon atoms in the sp^2-state in the samples of PND and DND nanopowders decrease as a result of their oxidation with atmospheric oxygen during annealing in air.

Thus, XPS and Raman spectroscopy methods, as well as the direct images obtained using high-resolution TEM, provide consistent results showing that during the annealing of PND and DND samples in air (starting from a temperature of 400°C), the selective removal of structural formations consisting primarily of non-diamond carbon in sp^2-state and amorphous carbon in sp^3-hybridized state.

Returning to Fig. 1, which shows the photographic images of nanopowders, let us note that the color of both the original samples of DND and PND nanopowder, and the samples annealed in air at t = 550°C correlates well with the relative content of structural formations of non-diamond carbon in sp^2- and sp^3-states in them. The high content of non-diamond car-

Table 7. **The weight losses of PND and DND samples depending on the temperature and duration of their annealing in air and the basic processes occurring in nanopowder samples**

Таблица 7. Потери массы образцов ПНА и ДНА в зависимости от температуры и длительности их отжига на воздухе и основные процессы, протекающие в образцах нанопорошков

t, °C	Time, h	Weight loss, %		The main processes occurring in the samples of diamond nanopowders during annealing in air
		PND	DND	
200	1	0.14	4.01	Desorption and removal of water molecules and volatile impurities [38–40]
300	2	0.30	5.08	
400	3	1.13	7.36	The oxidation of the smallest formations of non-diamond sp^2-carbon and amorphous carbon in the sp3-state [4, 7, 21–23]
500	5	3.08	14.21	The oxidation of graphite-like sp^2-carbon, amorphous carbon in the sp^3-state, and small primary particles of nanopowders [4, 7, 33]
550	6	5.37	21.09	

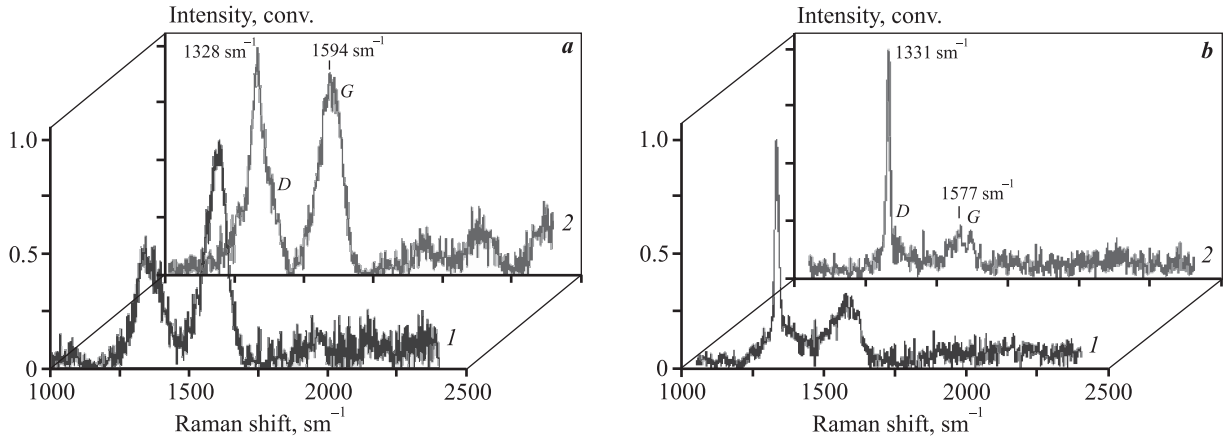

Fig. 8. The Raman spectra of the samples of PND (***a***) and DND (***b***) nanopowders before annealing (***1***) and after annealing in air at a temperature of 550 °C (***2***)

The spectra are adjusted by background subtraction and normalized to unity

Рис. 8. Спектры КР образцов нанопорошков ПНА (***a***) и ДНА (***b***) до отжига (***1***) и после отжига на воздухе при температуре 550 °C (***2***)

Спектры скорректированы путем вычитания фона и нормированы на единицу

bon in the original samples of diamond nanopowders contributes to their dark colour tint. The removal of structural formations of non-diamond carbon located both on the shell of the diamond core and in the space between adjacent primary particles during annealing in air causes a lighter color of PND and DND nanopowders.

The weight loss of samples of PND and DND nanopowders after their annealing in air. Table 7 shows that at an annealing temperature of 200 °C the weight loss of PND sample was 0.14 % of its initial value, and the weight loss of DND sample sample accounted for 4.01 %.

The relatively high weight loss of DND sample upon heating in air compared to the one of PND sample is apparently caused by the higher value of its specific surface area, which is capable of adsorbing more water molecules and volatile impurities in the initial state.

As a result of annealing at $t = 300$ °C, the weight losses of PND and DND samples compared to their initial values accounted for 0.3 % and 5.08 %, respectively. In

addition to the removal of adsorbed water molecules and volatile compounds, the weight losses at this annealing temperature might also be caused by desulfuring and denitrogenation, the presence of sulfur- and nitrogen-containing compounds in the original samples is associated with the chemical purification of the original nanopowders using the mixtures of strong acids, containing H_2SO_4 and HNO_3 [38, 39].

At t = 400 °C, the weight losses of PND and DND samples increase noticeably and account for 1.13 and 7.36 %, respectively. A noticeable increase in the weight losses is caused by the beginning of the processes of oxidation and removal of small structural formations consisting of non-diamond carbon in sp^2-state and amorphous carbon in sp^3-hybridized state [4, 7].

In the case of t = 500 °C and 550 °C, the weight losses of the original PND and DND samples increase significantly. After annealing at temperatures of 500°C and 550 °C, the original PND samples lost 3.08 % and 5.37 %, and the DND samples lost 14.21 % and 21.09 %, respectively. The increase in the weight losses of the samples at these temperatures is caused by active oxidation and removal of non-diamond carbon from them, which is reflected by the data of XPS and Raman spectra measurements, in particular, the change in the ratio of various forms of carbon sp^2/sp^3 (see Table 4).

Conclusion

A complex of modern methods was used in the course of the research aimed to study the impact of modification by annealing in air on the morphology, elemental and phase compositions, chemical state, and structure of primary particles of nanopowders obtained by the methods of grinding natural diamond and detonation synthesis. The annealing of nanopowder samples was performed at 5 given values of temperature: 200 °C, 300 °C, 400 °C, 500 °C and 550 °C.

It is shown that heat treatment in air at given values of temperature and heating time does not affect the elemental composition and atomic structure of primary particles of both DND and PND nanopowders. Using XPS and Raman spectroscopy methods, it has been established that annealing in air in the temperature range of 400—550 °C results in the removal of amorphous and graphite-like carbon atoms in sp^2- and sp^3-states from diamond nanopowders by oxidation with atmospheric oxygen. After annealing for 5 h at t = 550 °C, the relative number of non-diamond carbon atoms in the sp^2-state in the original DND nanopowder, containing about 33.2 % of non-diamond carbon atoms of the total number of carbon atoms, decreased to ~21.4 %. In this case, the relative number of carbon atoms in the sp3-state (in the diamond core lattice) and in the composition of oxygen-containing functional groups increased from ~39.8 % to ~46.5 % and from ~27 % to ~32.1 %, respectively. After annealing under the same conditions, their relative number in PND nanopowder, containing about 10.6 % of non-diamond carbon atoms in the sp^2-state of the total number of carbon atoms before annealing, decreased to 7.1 %. The relative number of carbon atoms in the sp^3-state increased from 72.9 to 82.1 %. The proportion of carbon atoms in the composition of oxygen-containing functional groups increased insignificantly (from 10.2 to 10.8 %) as well.

It is demonstrated that after annealing in air PND nanopowders exhibit a noticeable increase in the proportion of oxygen atoms in the composition of ester, carbonyl, and carboxyl functional groups compared to its content in the original sample, Whereas, in DND samples annealed in air, the proportion of oxygen atoms of the hydroxyl and carbonyl groups in the composition of ester, anhydride, and carboxyl groups somewhat decreases compared to the original sample. Besides, in DND samples after annealing, a slight increase in the proportion of oxygen atoms of the non-carbonyl group was recorded only in the composition of carboxyl, anhydride, and ester groups.

Acknowledgments: *The research was performed with the financial support from the Ministry of Education and Science of Russia within the frames of State Assignment for Project FSRG-2020-0017.*

Исследование выполнено при финансовой поддержке Минобрнауки России в рамках государственного задания по проекту FSRG-2020-0017.

References

1. *Долматов В.Ю.* Ультрадисперсные алмазы детонационного синтеза: свойства и применение. *Успехи химии*. 2001. Т. 70. No. 7. С. 687—708.
   Dolmatov V.Y. Detonation synthesis ultradispersed diamonds: properties and applications. *Russ. Chem. Rev.* 2001. Vol. 70. No. 7. P. 607—626. DOI: 10.1070/RC2001v070n07ABEH000665.
2. *Новиков Н.В., Богатырева Г.П., Волошин М.Н.* Детонационные алмазы в Украине. *Физика тв. тела*. 2004. Т. 46. No. 4. С. 585—590.
   Novikov N.V., Bogatyreva G.P., Voloshin M.N. Detonation

diamond in Ukraine. *Phys. Solid State*. 2004. Vol. 46. No. 4. P. 600—605. DOI: 10.1134/1.1711432.

3. *Верещагин А.Л.* Строение и реакционная способность детонационных алмазов. *Юж.-сиб. науч. вестн.* 2017. Т. 18. No. 2. С. 24—30. http://s-sibsb.ru/issues/51-2017-issues/issue-18/200-5.
   Vereshchagin A.L. Structure and reactivity of detonation diamonds. *Yuzhno-sibirskii nauchnyi vestnik*. 2017. Vol. 18. No. 2. P. 24—30 (In Russ.).
4. *Osswald S., Yuchin G., Mochalin V., Kucheyev S.O., Gogotsi Y.* Control of sp^2/sp^3 carbon ratio and surface chemistry of nanodiamond powders by selective oxidation in air. *J. Am. Chem. Soc.* 2006. Vol. 128. No. 35. P. 11635—11642. DOI: 10.1021/ja063303n.
5. *Плотников В.А., Демьянов Б.Ф., Макаров С.И., Черков А.Г.* Атомная структура нанокристаллов детонационного алмаза. *Фундам. пробл. соврем. материаловедения*. 2012. Т. 9. No. 4. С. 521—526.
   Plotnikov V.A., Dem'yanov B.F., Makarov S.I., Cherkov A.G. Atomic structure of detonation diamond nanocrystals. *Fundamental'nye problemy sovremennogo materialovedeniya*. 2012. Vol. 9. No. 4. P. 521—526 (In Russ.).
6. *Шарин П.П., Сивцева А.В., Яковлева С.П., Копырин М.М., Кузьмин С.А., Попов В.И., Никифоров Л.А.* Сравнение морфолических и структурных характеристик частиц нанопорошков, полученных измельчением природного алмаза и методом детонационного синтеза. *Известия вузов. Порошковая металлургия и функциональные покрытия*. 2019. No. 4. С. 55—67.
   Sharin, P.P., Sivtseva, A.V., Yakovleva, S.P., Kopyrin M.M., Kuz'min S.A., Popov V.I., Nikiforov L.A. Comparison of morphological and structural characteristics of nanopowder particles fabricated by grinding natural diamond and detonation synthesis. *Russ. J. Non-Ferr. Met.* 2020. Vol. 61. No. 4. P. 456—465. DOI: 10.3103/S1067821220040100.
7. *Stehlik S., Varga M., Ledinsky M., Jirasek V., Artemenko A., Kozak H, Ondic L., Skakalova V., Argentero G., Pennycook T., Meyer J.C., Fejfar A., Kromka A., Rezek B.* Size and purity control of HPHT nanodiamonds down to 1 nm. *J. Phys. Chem. C.* 2015. Vol. 119. No. 49. P. 27708—27720. DOI: 10.1021/acs.jpcc.5b05259.
8. *Плотников В.А., Демьянов Б.Ф., Макаров С.В., Богданов Д.Г.* Примесная подсистема детонационного наноалмаза. *Фундам. пробл. соврем. материаловедения.* 2013. Т. 10. No. 4. С. 487—492.
   Plotnikov V.A., Dem'yanov B.F., Makarov S.V., Bogdanov D.G. Impurity detonation nanodiamond subsystem. *Fundamental'nye problemy sovremennogo materialovedeniya*. 2013. Vol. 10. No. 4. P. 487—492 (In Russ.).
9. *Sharin P.P., Sivtseva A.V., Popov V.I.* X-rays photoelectron spectroscopy of nanodiamonds obtained by grinding and denotation synthesis. *Tech. Phys.* 2021. Vol. 66. No. 2. P. 275—279. DOI: 10.1134/S1063784221020183.
10. *Yongwei Zhu, Zhijing Feng, Baichun Wang, Xianyang Xu.* Dispersion of nanodiamond and ultra-fine polishing of quartz wafer. *China Particuology*. 2004. Vol. 2. No. 4. P. 153—156. DOI: 10.1016/S1672-2515(07)60046-3.
11. *Hirata A., Igarashi M., Kaito T.* Study on solid lubricant properties of carbon onion produced by heat treatment of diamond cluster or particles. *Tribol. Int.* 2004. Vol. 39. P. 899—905. DOI:10.1016/j.triboint.2004.07.006.
12. *Zhao X., Wang T., Li Y., Huang L., Handschuh-Wang S.* Polydimethylsiloxane/nanodiamond composite sponge for enhanced mechanical or wettability performance. *Polymers*. 2019. Vol. 11. No. 6. P. 948—960. DOI: 10.3390/polym11060948.
13. *Afandi A., Howkins A., Boyd I., Jackman R.* Nanodiamonds for device applications: An investigation of the properties of boron-doped detonation nanodiamonds. *Sci. Rep.* 2018. Vol. 8. No. 1. P. 1—10. DOI: 10.1038/s41598-018-21670-w.
14. *Hsu S-H., Kang W.P., Davidson J.L., Huang J.H., Kerns D.V. Jr.* Nanodiamond vacuum field emission integrated differential amplifier. *IEEE Trans. Electron Devices*. 2013. Vol. 60. No. 1. P. 487—493. DOI: 10.1109/TED.2012.2228485.
15. *Тверитинова Е.А., Житнев Ю.Н., Кулакова И.И., Маслаков К.И., Нестерова Е.А., Харланов А.Н., Иванов А.С., Савилов С.В., Лунин В.В.* Влияние структуры и свойств поверхности на каталитическую активность наноалмаза в конверсии 1,2-дихлорэтана. *Журн. физ. химии*. 2015. Т. 89. No. 4. С. 680—687.
   Tveritinova E.A., Zhitnev Yu.N, Kulakova I.I., Maslakov K.I., Nesterova E.A., Kharlanov A.N., Ivanov A.S., Savilov S.V., Lunin V.V. Effect of structure and surface properties on the catalytic activity of nanodiamond in the conversion of 1,2-dichloroethane. *Russ. J. Phys. Chem. A.* 2015. Vol. 89. No. 4. P. 680—687. DOI: 10.1134/S0036024415040251.
16. *Lin Y., Sun X., Su D., Centi G., Perathoner S.* Catalysis by hybrid sp^2/sp^3nanodiamonds and their role in the design of advanced nanocarbon materials. *Chem. Soc. Rev. 2018*. Vol. 47. No. 22. P. 8438—8473. DOI: 10.1039/C8CS00684A.
17. *Яковлев Р.Ю., Соломатин А.С., Леонидов Н.Б., Кулакова И.И., Лисичкин Г.В.* Детонационный наноалмаз — перспективный носитель для создания систем доставки лекарственных веществ. *Рос. хим. журн.* 2012. Т. 56. No. 3—4. С. 114—125.

Yakovlev R.Yu., Solomatin A.S., Leonidov N.B., Kulakova I.I., Lisichkin G.V. Detonation nanodiamond — a perspective carrier for drug delivery systems. *Russ. J. Gen. Chem.* 2014. Vol. 84. No. 2. P. 379—390. DOI: 10.1134/S1070363214020406.

18. *Huang H., Pierstorff E., Ho D., Osawa E.* Active nanodiamond hydrogels for chemotherapeutic delivery. *Nano Lett.* 2007. Vol. 7. No. 11. P. 3305—3314. https://doi.org/10.1021/nl071521o.
19. *Schrand A.M., Dai L., Schlager J.J., Hussain S.M., Osawa E.* Differential biocompatibility of carbon nanotubes and nanodiamonds. *Diam. Relat. Mater.* 2007. Vol. 16. No. 12. P. 2118—2123. https://doi.org/10.1016/j.diamond.2007.07.020.
20. *Tsai L.-W., Lin Y.-C., Perevedentseva E., Lugovtsov A., Priezzhev A., Cheng C.-L.* Nanodiamonds for medical applications: interaction with blood in vitro and in vivo. *Int. J. Mol. Sci.* 2016. Vol. 17. No. 7. P. 1111 (17). DOI: 10.3390/ijms17071111.
21. *Денисов С.А., Дзидзигури Э.Л., Спицын Б.В., Соколина Г.А., Болдырев Н.Ю.* Очистка и модификация продукта детонационного синтеза алмаза. *Уч. записки Петрозав. гос. ун-та. Сер. Физ.-мат. науки.* 2011. No. 2. С. 89—98.
Denisov S.A., Dzidziguri E.L., Spitsyn B.V., Sokolina G.A., Boldyrev N.Y. Purification and modification of the product of detonation synthesis of diamond. *Uchenye zapiski Petrozavodskogo gos. un-ta. Ser. Fiziko-matematicheskie nauki*. 2011. No. 2. P. 89—98 (In Russ.).
22. *Чиганов А.С.* Селективное ингибирование окисления наноалмазов в технологии очистки. *Физика тв. тела*. 2004. Т. 46. No. 4. С. 605—606.
Chiganov A.S. Selective inhibition of the oxidation of nanodiamonds for their cleaning. *Phys. Solid State.* 2004. Vol. 46. No. 4. P. 620—621. https://doi.org/10.1134/1.1711436.
23. *Korepanov V.I., Hamaguchi H., Osawa E., Ermolenkov V., Lednev I., Etzold B., Levinson O., Zousman B., Eprella C.P., Chang H-C.* Carbon structure in nanodiamonds elucidated from Raman spectroscopy. *Carbon.* 2017. No. 121. P. 322—329. https://doi.org/10.1016/j.carbon.2017.06.012.
24. *Scofield J.H.* Hartree-slater subshell photoionization cross-sections at 1254 and 1487 eV. *J. Electron Spectrosc. Relat. Phenom.* 1976. Vol. 8. No. 2. P. 129—137. DOI: 10.1016/0368-2048(76)80015-1.
25. *Орлов Ю.Л.* Минералогия алмаза. 2-е изд. М.: Наука, 1984.
Orlov Yu.L. Diamond mineralogy. Moscow: Nauka, 1984 (In Russ.).
26. *Гурин В.А., Габелков С.В., Полтавцев Н.С., Гурин И.В., Фурсов С.Г.* Кристаллическая структура пирографита и каталитически осажденного углерода. *Вопр. атом. науки и техники. Сер. Физика радиац. повреждений и радиац. материаловедение.* 2006. Т. 89. No. 4. С. 195—199.
Gurin V.A., Gabelkov S.V., Poltavtsev N.S., Gurin I.V., Fursov S.G. Crystal structure of pyrographite and catalytically deposited carbon. *Voprosy atomnoi nauki i tekhniki. Ser. Fizika radiatsionnykh povrezhdenii i radiatsionnoe materialovedenie.* 2006. Vol. 89. No. 4. P. 195—199 (In Russ.).
27. *Штольц А.К., Медведев А.И., Курбатов Л.В.* Рентгеновский анализ микронапряжений и размера областей когерентного рассеяния в поликристаллических материалах. Екатеринбург: УГТУ—УПИ, 2005. https://study.urfu.ru/Aid/Publication/328/1/Shtolts_Medvedev_Kurbatov.pdf
Shtols A.K., Medvedev A.I., Kurbatov L.V. X-ray analysis of microstresses and sizes of coherent scattering regions in polycrystalline materials. Ekaterinburg: UGTU—UPI, 2005 (In Russ.).
28. *Андреев В.Д., Созин Ю.И.* Структура ультрадисперсных алмазов. *Физика тв. тела.* 1999. Т. 41. No. 10. С. 1890—1892.
Andreev V.D., Sozin Y.I. Structure of ultradisperse diamonds. *Phys. Solid State.* 1999. Vol. 41. No. 10. P. 1736—1739. https://doi.org/10.1134/1.1131077.
29. http://xpspeak.software.informer.com/4.1.
30. *Алексенский А.Е., Осипов В.Ю., Вуль А.Я., Бер Б.Я., Смирнов А.Б.* Оптические свойства слоев наноалмазов. *Физика тв. тела.* 2001. Т. 43. No. 1. С. 140—145.
Aleksenskii A.E., Osipov V.Y., Vul' A.Y., Ber B.Y., Smirnov A.B. Optical properties of nanodiamond layers. *Phys. Solid State*. 2001. Vol. 43. No. 1. P. 145—150. DOI: 10.1134/1.1340200.
31. *Fang C., Zhang Yu., Shen W., Sun Sh., Zhang Zh., Xue L., Jia X.* Synthesis and characterization of HPHT large single-crystal diamonds under the simultaneous influence of oxygen and hydrogen. *Cryst. Eng. Comm*. 2017. Vol. 19. No. 38. P. 5727—5734. DOI: 10.1039/C7CE01349C.
32. *Qi M., Xiao J., Cheng Y., Wang Zh., Jiang A., Guo Y., Tao Z.* Effect of various nitrogen flow ratios on the optical properties of (Hf : N)—DLC films prepared by reactive magnetron sputtering. *AIP Adv.* 2017. Vol. 7. No. 8. P. 085012. DOI: 10.1063/1.4993631.
33. *Швидченко А.В., Жуков А.Н., Дидейкин А.Т., Байдакова М.В., Шестаков М.С., Шнитов В.В., Вуль А.Я.* Электрические свойства поверхности монокристаллических частиц детонационного наноалмаза, полученных отжигом агломератов в атмосфере воздуха. *Коллоид. журн*. 2016. Т. 78. No. 2. С. 218—224. DOI: 10.7868/S0023291216020142.

Shvidchenko A.V., Zhukov A.N., Dideikin A.T., Baidakova M.V., Shestakov M.S., Shnitov V.V., Vul' A.Ya. Electrical properties of the surface of single-crystal particles of detonation nanodiamond obtained by annealing agglomerates in air. *Kolloidnyi Zhurnal*. 2016. Vol. 78. No. 2. P. 218—224 (In Russ.).

34. *Araùjo M.P., Soares O.S.G.P., Fernandes A.J.S., Pereira M.F.R., Freire C.* Tuning the surface chemistry of graphene flakes: new strategies for selective oxidation. *RSC Adv*. 2017. No. 7. P. 14290. DOI: 10.1039/c6ra28868e.
35. *Li H., Xu T., Wang C., Chen J., Zhou H., Liu H.* Effect of relative humidity on the tribological properties of hydrogenated diamond-like carbon films in a nitrogen environment. *J. Phys. D: Appl. Phys.* 2005. Vol. 38. P. 62—69. DOI: 10.1088/0022-3727/38/1/011.
36. *Полянская Е.М., Таран О.П.* Исследование функциональных групп на поверхности окисленного углеродного материала Сибунит методами кислотно-основного титрованияи РФЭС. *Вестн. Томск. гос. ун-та. Химия.* 2017. No. 10. С. 6—26. DOI: 10.17223/24135542/10/1.
Polyanskaya E.M., Taran O.P. Study of functional groups on the surface of the oxidized carbon material Sibunit by acid-base titration and XPS. *Vestnik Tomskogo gos. un-ta. Khimiya*. 2017. No. 10. P. 6—26 (In Russ.).
37. *Rey A., Faraldos M., Bahamonde A., Casas J.A., Zazo J.A., Rodríguez J.J.* Role of the activated carbon surface on catalytic wet peroxide oxidation. *Ind. Eng. Chem. Res.* 2008. Vol. 47. No. 21. P. 8166—8174. DOI: 10.1021/ie800538t.
38. *Богданов Д.Г., Макаров С.В., Плотников В.А.* Десорбция примесей при нагреве детонационного наноалмаза. *Письма в ЖТФ*. 2012. Т. 38. No. 4. С. 89—95.
Bogdanov D.G., Makarov S.V., Plotnikov V.A. Thermodesorption of impurities from detonation nanodiamond. *Tech. Phys. Lett.* 2012. Vol. 38. No. 4. P. 199—202. https://doi.org/10.1134/S1063785012020198.
39. *Плотников В.А., Богданов Д.Г., Макаров С.В., Богданов А.С.* Сорбционные и десорбционные свойства детонационного наноалмаза. *Изв. вузов. Химия и хим. технология*. 2017. Т. 60. No. 9. С. 27—32. DOI: 10.6060/tcct.2017609.1y.
Plotnikov V.A., Bogdanov D.G., Makarov S.V., Bogdanov A.S. Sorption and desorption properties of detonation nanodiamond. *Izvestiya vuzov. Khimiya i khimicheskaya tekhnologiya*. 2017. Vol. 60. No. 9. P. 27—32 (In Russ.).
40. *Кощеев А.П., Горохов П.В., Громов М.Д., Перов А.А., Отт У.* Химия поверхности модифицированных детонационных наноалмазов различных типов. *Журн. физ. химии*. 2008. Т. 82. No. 10. С. 1908—1914.
Koshcheev A.P., Gorokhova P.V., Gromova M.D., Perova A.A., Ott U. The chemistry of the surface of modified detonation nanodiamonds of different types. *Russ. J. Phys. Chem. A*. 2008. Vol. 82. No. 10. P. 1708—1714. DOI: 10.1134/S0036024408100129.